Rate-induced tipping in natural and human systems

Paul Ritchie[1], Hassan Alkhayuon[2], Peter Cox[1], and Sebastian Wieczorek[2]

[1]College of Engineering, Mathematics and Physical Sciences, University of Exeter, North Park Road, Exeter, EX4 4QE, UK.
[2]School of Mathematical Sciences, University College Cork, Western Road, Cork T12 XF62, Ireland.

Correspondence: Paul Ritchie (Paul.Ritchie@exeter.ac.uk)

Abstract. Over the last two decades, tipping points have become a hot topic due to the devastating consequences that they may have on natural and human systems. Tipping points are typically associated with a system bifurcation when external forcing crosses a *critical level*, causing an abrupt transition to an alternative, and often less desirable, state. The main message of this review is that the *rate of change* in forcing is arguably of even greater relevance in the human-dominated anthropocene, but is rarely examined as a potential sole mechanism for tipping points. Thus, we address the related phenomenon of rate-induced tipping: an instability that occurs when external forcing varies across some *critical rate*, usually without crossing any bifurcations. First, we explain when to expect rate-induced tipping. Then, we use three illustrating examples of differing complexity to highlight universal and generic properties of rate-induced tipping in a range of natural and human systems.

1 Introduction

Large abrupt changes may occur in open non-linear systems when the external forcing exceeds some *critical level* (Scheffer, 2010; Lenton, 2011; Kuehn, 2011). Such changes are commonly referred to as *bifurcation-induced tipping points* (Ashwin et al., 2012). They have been identified in many domains, including ecosystems (Scheffer et al., 2009; Dakos et al., 2019) and the human brain (Maturana et al., 2020), and are of particular concern under anthropogenic climate change (Lenton et al., 2008; Ashwin and von der Heydt, 2020; Arias et al., 2021; Ritchie et al., 2021). Furthermore, it has recently been recognised that critical levels can be exceeded temporarily without causing tipping (van der Bolt et al., 2018; Ritchie et al., 2019; Alkhayuon et al., 2019; O'Keeffe and Wieczorek, 2020). This occurs when the time of exceedance is short compared to the inherent timescale of the system (O'Keeffe and Wieczorek, 2020; Ritchie et al., 2021; Alkhayuon et al., 2022).

However, there is another, less obvious potential consequence of changes in external forcing. When an external forcing changes fast enough, rather than necessarily by a large amount, this can lead to *rate-induced tipping points* (Luke and Cox, 2011; Wieczorek et al., 2011; Ashwin et al., 2012; Ritchie and Sieber, 2016; Siteur et al., 2016; Suchithra et al., 2020; Wieczorek et al., 2021; Longo et al., 2021; Kuehn and Longo, 2022; Kaur and Sharathi Dutta, 2022; Hill et al., 2022). In contrast to bifurcation-induced tipping, rate-induced tipping usually occurs without exceeding any critical levels by external forcing. Such tipping points are much less widely known, and yet are arguably even more relevant to contemporary issues such as climate change (Lohmann and Ditlevsen, 2021; Clarke et al., 2021; O'Sullivan et al., 2022), ecosystem collapse (Scheffer et al., 2008; Vanselow et al., 2019; van der Bolt and van Nes, 2021; Neijnens et al., 2021; Vanselow et al., 2022), and the resilience of human systems (Witthaut et al., 2021).
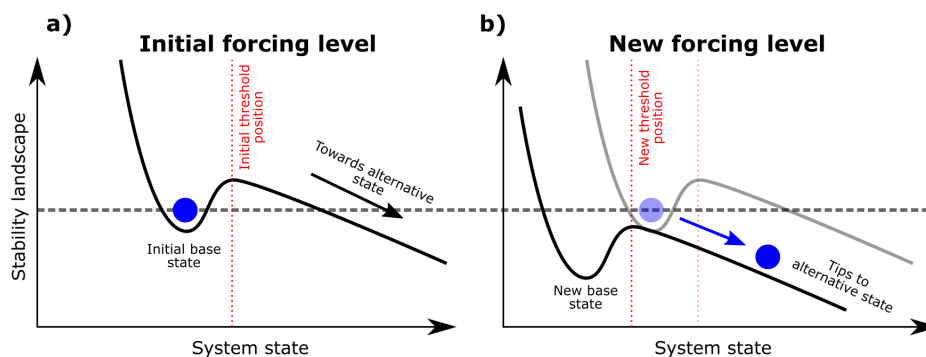
Figure 1. Schematic illustration of threshold instability. (a) The stability landscape of the system at an initial level of forcing. The well represents the base state, the hill top defines the threshold (indicated by the red dashed vertical line), and the (blue) ball indicates the current state of the system. To the left of the hill top (threshold), the ball rolls into the well, meaning the system converges to the base state. To the right of the hill top, the ball runs away, indicating tipping to an alternative state. (b) The stability landscape at a new forcing level. Note that the initial base state is on the other side of the new hill top (threshold). Therefore, if the system is at the initial base state and the forcing switches instantaneously to the new level, the ball will run away, meaning the system will tip to an alternative state.

This review makes the concept of rate-induced tipping points accessible to a wide scientific audience. Even though the phenomenon is rarely discussed by scientists and policy makers, we argue that it is ubiquitous and likely to be prevalent in many forced systems. We demonstrate this through analysis of three models of natural and human systems with differing complexity: a predator-prey ecosystem; the large-scale ocean circulation; and an electrical power grid network. Easily verifiable criteria for the occurrence of rate-induced tipping, such as *threshold instability* and *basin instability*, as well as universal features including multiple *critical rates of change* related to *return tipping*, are identified in all of these examples.

2   When to expect Rate-induced tipping?

A system is known to be susceptible to rate-induced tipping if the state the system currently resides in is *threshold unstable* (O'Keeffe and Wieczorek, 2020; Wieczorek et al., 2021). One way of depicting threshold instability is with a moving stability landscape, as illustrated by Figure 1.[1] For a given initial level of external forcing the system is assumed to be at a stable equilibrium (though in general it can be a stable limit cycle or an even more complicated attractor) referred to as the *base state*, and is represented by the blue ball in the well in panel (a). The hill top defines the position of the *threshold* (indicated by the vertical red dashed line). If the ball is to the left of the hill top (threshold), it will roll into the well and the system will converge to the base state. Whereas, if the ball is to the right of the hill top, it will roll in the opposite direction and the system will tip to some *alternative state*. The alternative state may be a *different stable state* for a multistable system (Scheffer et al., 2008; O'Keeffe and Wieczorek, 2020; Halekotte and Feudel, 2020; Lohmann et al., 2021; Slyman and Jones, 2022), or a

---

[1]Note that not all systems can be characterised by a stability landscape.

transient state for an excitable (possibly monostable) system (Wieczorek et al., 2011; Vanselow et al., 2019; O'Sullivan et al., 2022).

45   In contrast to bifurcation-induced tipping, the change in the forcing usually does not cause any qualitative change in the stability landscape but instead shifts its position. If the threshold moves past the initial position of the well for a new forcing level, as shown in panel (b), the base state is said to be *threshold unstable* on varying the forcing (Wieczorek et al., 2021). In the case when the threshold is a basin boundary of two attractors in a multistable system, the system is said to be *basin unstable* (O'Keeffe and Wieczorek, 2020). One can prove that, in general, threshold instability is sufficient for the occurrence

50   of rate-induced tipping (Kiers and Jones, 2020; Wieczorek et al., 2021). However, in many examples including those considered here, threshold instability appears to be both necessary and sufficient for the occurrence of rate-induced tipping. This can be understood as follows. If the forcing changes at a vanishing rate, the ball remains in the well and the system is said to *track* the moving base state. If the forcing switches instantaneously, the initial ball finds itself on the other side of the hill top (threshold) and tips to an alternative state. Thus, there will be a forcing that changes continuously from the initial level to the new level

55   and causes the system to rate-tip to an alternative state above some *critical rate of change*. Once it is known that a system is susceptible to rate-induced tipping, the goal is to find the critical rate, or even multiple critical rates, for a given shape of continuous external forcing.

3   Rate-induced tipping in a simple model

In natural and human systems, tipping points are often associated with crossing a critical level of the forcing, defined by a

60   dangerous (e.g. fold) bifurcation, causing a catastrophic, abrupt and irreversible change to the state of the system (Thompson et al., 1994; Thompson and Sieber, 2011). This type of tipping is commonly referred to as bifurcation-induced tipping (or B-tipping) and is illustrated by Figure 2(a) (Ashwin et al., 2012). Suppose the system starts on the upper branch of stable equilibria as indicated by the grey dot. Initially, as external forcing changes slowly, the state of the system (the red trajectory in Figure 2 (a)) tracks the branch of stable equilibria. However, once external forcing reaches the fold that defines the critical

65   level of the forcing, the upper stable branch terminates and the system subsequently undergoes a catastrophic transition to the alternative stable state. Crucially, the tipping occurs for any rate of change of the forcing past the Fold. The alternative state is often a less desired state, such as an extinction state in an ecosystem (O'Keeffe and Wieczorek, 2020), collapse of an ocean circulation (Alkhayuon et al., 2019), or a blackout on a power grid network (Budd and Wilson, 2002). However, it could also be a more desired state, such as a well-being state for developing countries (Mirza et al., 2019).

70   Figure 2 introduces a subtle but crucial difference to previous examples that have considered B-tipping (Lenton et al., 2008; Scheffer et al., 2009; Ritchie et al., 2021) and that is to apply a tilt to the bifurcation structure (O'Keeffe and Wieczorek, 2020, Sec.7). This important distinction introduces the possibility of a different form of tipping known as rate-induced tipping (or R-tipping). Unlike B-tipping in Figure 2(a), where crossing a critical level of the external forcing causes a catastrophic transition, R-tipping occurs when the system fails to adapt to a too rapidly changing external forcing, usually without crossing

75   any critical levels. Figure 2(b) considers two scenarios where external forcing is changed by the same extent, but at different
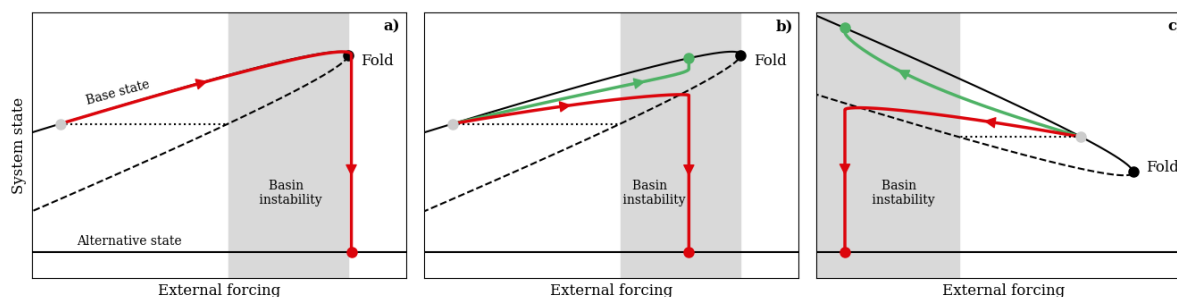
Figure 2. Illustration of bifurcation-induced, rate-induced, and return tipping. (a) Bifurcation-induced tipping: slow change in external forcing past a critical level (Fold bifurcation) causes tipping. The tipping occurs for any rate of change of the forcing past the Fold. (b) Rate-induced tipping: the system fails to adapt to a fast change in external forcing (red) even though the forcing never crosses the critical level. For a slow enough change of the forcing the system tracks the moving base state and avoids tipping (green). (c) Return tipping: avoiding bifurcation-induced tipping by reversing the trend in the external forcing too quickly can lead to rate-induced tipping on decrease of the forcing. Branches of stable equilibria are denoted by black solid curves, and branches of unstable equilibria are denoted by black dashed curves. Stable and unstable branches meet at a Fold bifurcation (black dot). The system starting from the grey dot is basin unstable for forcing shift magnitudes that end in the grey region of basin instability.

rates. Most importantly, the forcing stops in the (grey) region of basin istability, and never crosses the critical level defined by the Fold bifurcation point. For a slow rate of change in external forcing (green trajectory), the system is able to continually adapt to the moving base state and tracks the stable branch of equilibria without tipping. However, for a slightly faster rate of change in external forcing (red trajectory), the system is unable to adapt to the moving base state and undergoes R-tipping.

80   If a system is thought to be approaching a B-tipping event, then a natural option would be to reverse the external forcing to avoid crossing the critical level. However, fast reversals in the forcing introduce a new problem that has been largely overlooked, namely *return tipping* (O'Keeffe and Wieczorek, 2020). Figure 2(c) illustrates such a scenario for a Fold bifurcation structure tilted down. Suppose that external forcing has caused a system to approach close to the Fold bifurcation. Reversing the forcing slowly will allow the system to closely track the stable equilibrium branch as shown by the green trajectory. However, a too

85 fast reversal may give rise to R-tipping on return if the system is basin unstable on reversal of the forcing. Then, the end result is opposite to what was intended. Although B-tipping is avoided, the system, rather surprisingly, R-tips to the alternative stable state (red trajectory). Therefore, in general, reversing external forcing as quickly as possible does not guarantee avoiding tipping.

        Let us assume initially that the external forcing takes the form of a *nonlinear shift ramp* trajectory, see Methods for details.

90 Three sample time series that undergo a ramp shift at different rates but between the same levels in external forcing are given by a concatenation of the left half of a colour curve and the black dashed curve in Figure 3(a). The corresponding response of the system subject to these external forcing trajectories is depicted in Figure 3(b). For the slowest change in external forcing (the blue dashed trajectory) the system is able to adapt to and track the changing base state. However, if the rate of change in
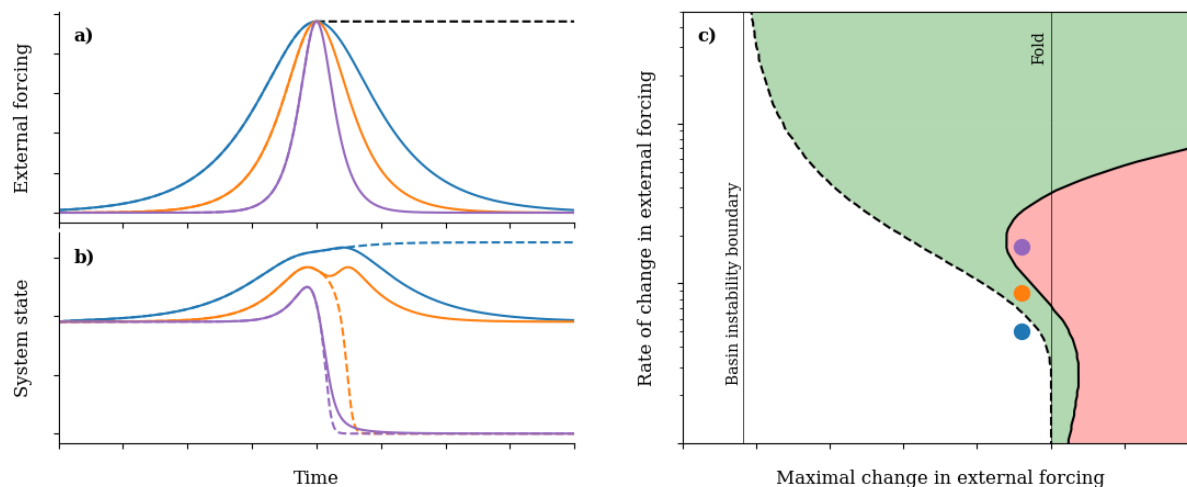
Figure 3. Tipping for a nonlinear shift ramp and return profiles in the tilted fold example. Time series of external forcing (a) and system response (b) for ramp (dashed) and return (solid) forcing profiles. Forcing profiles vary between same minimum and maximum levels but at different rates: slow (blue), medium (orange) and purple (fast). (c) Tipping diagram for ramp and return profiles. Critical boundaries separate regions of tracking from tipping for the ramp profile (black dashed curve) and for return profile (solid black curve). White region: tracking for ramp and return profiles; green region: tipping for ramp profile, tracking for return profile; red region: tipping for ramp and return profiles.

external forcing becomes too fast (the orange and purple dashed trajectories), then the system fails to adapt to the changing
95   base state and R-tips to the alternative state.

The critical rate, which determines the onset of R-tipping, will depend on how much the external forcing is changed by. The black dashed curve in Fig. 3(c) shows the critical boundary separating regions of tipping (coloured) from no tipping (white), in the plane of the rate of change against the maximal change, for the ramp external forcing. Previous research has shown that B-tipping occurs if the ramp external forcing crosses the Fold bifurcation. Indeed, for slow rates the critical boundary
100   asymptotes to the distance required to reach the Fold (indicated by the thin black line). However, for faster rates, tipping can occur before the Fold is transgressed because of R-tipping. The coloured dots correspond to the external forcing parameters used in Figure 3(a) and (b). Notice that the blue dot is in the white region, signifying tracking, whereas the other two dots are within the coloured regions denoting tipping. For large rates, the critical boundary asymptotes to the basin instability boundary: the smallest magnitude of an instantaneous switch in external forcing that gives basin instability as described in Figure 1.

105   The green (points of return) region corresponds to scenarios where tipping is prevented if the external forcing is reversed back to its initial level after reaching its maximal level of change (see Methods for further details). The red (points of no return) region corresponds to scenarios where tipping still occurs despite reversing the external forcing. Previously, it has been shown for B-tipping that safely overshooting a critical level by a given distance can be achieved, provided the reversal in external forcing is faster than some critical rate. However, the possibility of R-tipping means that *multiple critical rates* can be defined

110 for return forcing with the same maximal change as the slow rates required to avoid R-tipping compete against the fast rates

required for safe overshoots. This is illustrated in Figure 3(c) by the solid black curve.

For a fixed maximal change in the ramp forcing, past the basin instability boundary and below the Fold level, there exists a

single critical rate and an interval of rates where R-tipping is caused by the forcing. In the green region, reversing the forcing

prevents the system from an impending R-tipping that would occur if the forcing were not to be reversed. An example is given

115 by the solid orange curve in Figure 3(b). Close to the Fold (the red region to the left of the vertical Fold line), there are two

critical rates bounding a (red) sub-interval of rates where this R-tipping is not prevented by return forcing. This is illustrated

by the purple solid curve in Figure 3(b).

For small overshoots of the Fold, even greater complexity is possible with the potential of three critical rates and two tipping

intervals for a single fixed maximal change of return forcing. At extremely slow rates (the red region to the right of the lower

120 part of the vertical Fold line), B-tipping occurs and cannot be prevented by reversing the forcing. However, for a faster reversal

in the forcing (the green region to the right of the lower part of the vertical Fold line), it becomes possible to prevent B-tipping

and avoid R-tipping upon return. However, increasing the rate even more (the red region to the right of the middle part of the

vertical Fold line) prevents B-tipping but triggers R-tipping, meaning that the system tips again despite reversing the forcing.

Then, for even higher rates (the green region to the right of the upper part of the vertical Fold line), both B-tipping and R-tipping

125 upon return can be prevented since the system does not have sufficient inertia to react to a short forcing impulse.

4 Rate-induced tipping in ecology and climate

We first consider an example from ecology, namely that of a predator-prey system, which models the time evolution of plant

and herbivore biomass densities (Scheffer et al., 2008; O'Keeffe and Wieczorek, 2020).

In this example, changes in environmental conditions affect the plant growth rate and herbivore mortality rate simultaneously,

130 and play the role of external forcing. Such a scenario can be considered possible under climate change, where plants benefit

from the fertilisation effect due to increasing levels of CO_2 (Reich et al., 2014), but the resulting increased temperatures are

detrimental to herbivores (Lacetera, 2019). The plant growth rate and herbivore mortality rate vary within a range where the

ecosystem has two stable equilibria. The stable coexistence equilibrium is the base state. The stable plant-only equilibrium

with no herbivores is the alternative stable state.

135 Three sample time profiles of ramp forcing are presented in Figure 4(a) that all increase the environmental conditions from

zero to one but at different rates. The resulting impacts on the herbivore biomass are shown in Figure 4(b). For the slowest

(green) change in environmental conditions, the ecosystem tracks the moving base state. Herbivores increase slightly, which

represents the continued presence of coexisting plants and herbivores. Contrast this to the fastest (red) change in environmental

conditions, which causes R-tipping to the alternative stable state. In this scenario, herbivore population declines to zero and the

140 ecosystem becomes entirely dominated by plants.

Figure 4(c) illustrates the underlying dynamics in the phase plane of the plant and herbivore biomass. For the initial level of

external conditions, the base state is indicated by the grey dot. The shift in the environmental conditions changes the position
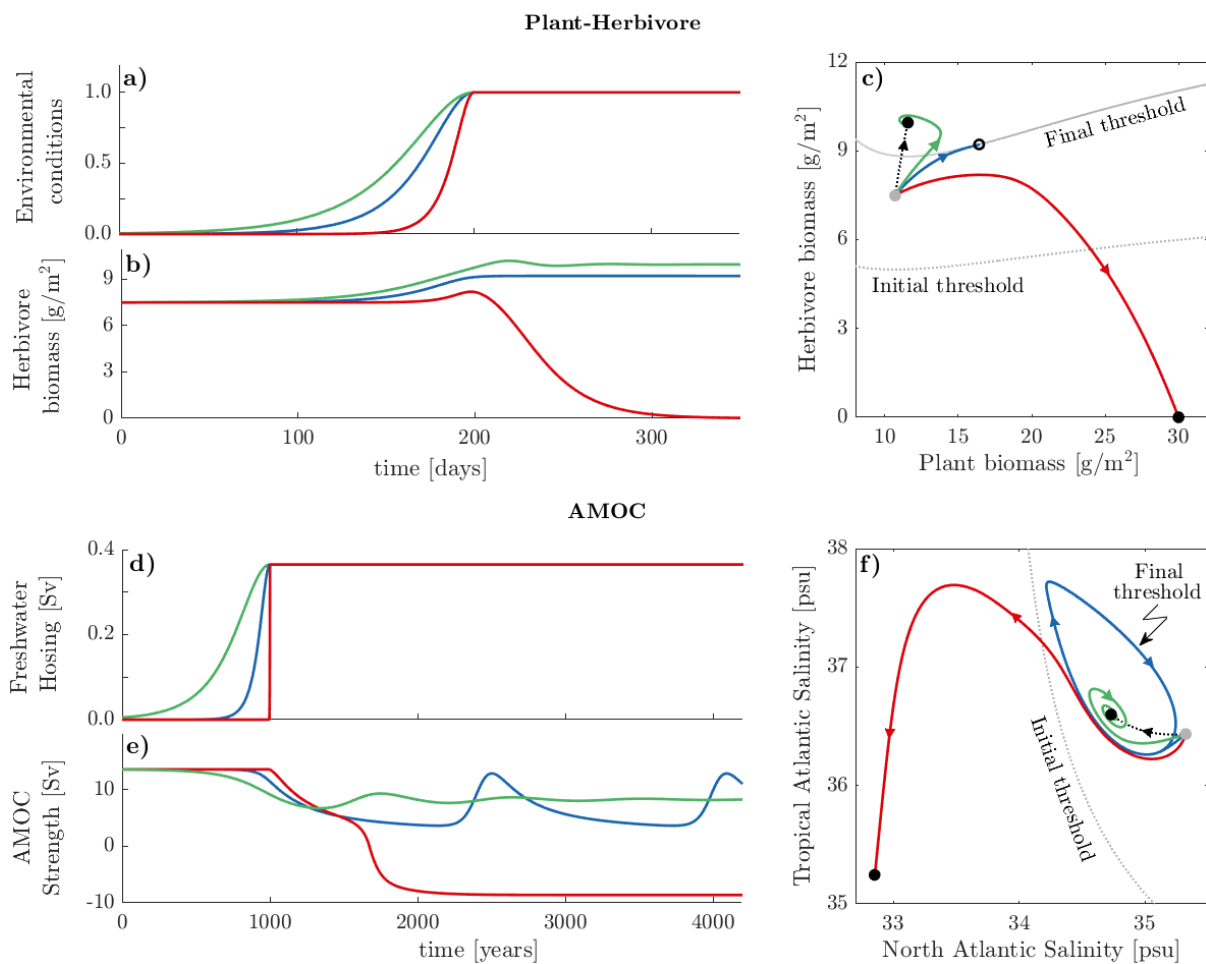
Figure 4. Rate-induced tipping in the plant-herbivore (top row) and AMOC (bottom row) models. Time series of the external forcing profiles: dimensionless environmental conditions (a) and freshwater hosing (d); see Methods for further details. The system responses to the changing environmental conditions (b) and freshwater hosing (e), for three different rates of change (different colours). The system responses in the phase plane of the plant and herbivore biomass (c), and the North and Tropical Atlantic salinities (f). See Supplementary Video 1 and Supplementary Video 2 for animated versions of (a)–(c) and (d)–(f) respectively.

of the base state, and this change is indicated by the dotted black line. The black dot at the other end of the dotted line indicates the base state for the final level of environmental conditions. Further ramifications of the shift in environmental conditions

145 include changes in the basin of attraction of the base state. The basin of attraction shifts (from the dotted curve to the solid grey curve) such that the initial base state (the grey dot) is not contained in the basin of attraction of the final base state (the region above the solid grey curve). A consequence of basin instability is that the behaviour of solutions starting near the initial base state depends on the rate of change of environmental conditions as follows. For slow rates, the system is able to continually adapt and remain within the changing basin of attraction of the base state so that solutions converge to the final base state; see

150 the green trajectory. However, for a sufficiently fast change, the ecosystem fails to track the fast moving base state and R-tips to the final alternative stable state indicated by the second black dot; see the red trajectory. This rate-sensitive behaviour is expected due to basin instability. What may be surprising is that, at a critical rate of change in environmental conditions, the corresponding solution converges to an unstable *edge state* (black circle) (Wieczorek et al., 2021) on the basin boundary of the final base state; see the blue trajectory.

155 Next, we consider an example from climate, specifically the possible collapse of the Atlantic Meridional Overturning Circulation (AMOC) under global warming. The AMOC forms part of the global thermohaline circulation, which is a large-scale ocean circulation current driven by temperature and salinity gradients. The AMOC contributes to the relatively mild climate in Western Europe by transporting heat from the Tropics to the North Atlantic. Once the warm salty waters reach the North Atlantic, they cool down and become denser. The higher density of these waters causes sinking (or overturning), followed by

160 a return to the Tropics along the bottom of the ocean. However, the AMOC can be easily disturbed by contemporary climate change. The amount of freshwater added to the North Atlantic (referred to as freshwater hosing) may increase under climate change, for example due to the melting of the Greenland Ice Sheet, changes in precipitation patterns, or both. Such an increase can cause a decrease in the salinity of the North Atlantic waters, making them less dense. This, in turn, may disrupt the overturning and potentially lead to a collapse of the AMOC (Wood et al., 2019; Lohmann and Ditlevsen, 2021). We describe the

165 dynamics of the AMOC using a global oceanic box model (Alkhayuon et al., 2019; Wood et al., 2019), in which changes in the freshwater hosing play the role of external forcing. The forcing varies within a range where the AMOC model has two stable equilibria. The stable AMOC-On equilibrium is the base state. The stable AMOC-Off equilibrium is the alternative stable state.

Figure 4(d) shows three sample time profiles of ramp forcing that increase the freshwater hosing from zero to the same non-zero level, but each at a different rate. The response of the AMOC to these freshwater forcing scenarios is shown in Figure 4(e).

170 For the slowest (green) change in freshwater hosing, there is tracking of the moving base state. The AMOC strength suffers a slight drop, but ultimately remains in the AMOC-On state. However, for the fast (red) change in freshwater hosing, there is R-tipping to the alternative stable state. The AMOC strength declines to a point of complete collapse.

The phase portrait in the plane of the salinities in the North and Tropical Atlantic boxes in Figure 4(f) illustrates the underlying dynamics . The grey dot shows the base state for the initial level of freshwater hosing. Increasing the freshwater hosing

175 shifts the base state as indicated by the black dotted line. The black dot at the other end of the dotted line indicates the base state at the final level of freshwater hosing. Notice that the basin of attraction of the final base state (the region enclosed by the blue periodic orbit) does not contain the initial base state (the grey dot). Therefore, the initial base state is basin unstable, and

R-tipping from the base state to the alternative stable state (lower black dot) will occur for sufficiently fast shifts in freshwater hosing. For slow rates, the system continually adapts and remains within the changing basin of attraction of the base state so

180 that solutions converge to the final base state; see the green trajectory. On the other hand, for sufficiently fast rates, the system is unable to adapt and falls outside the changing basin of attraction of the base state, causing solutions to converge to the final alternative state; see the red trajectory. At the critical rate of freshwater hosing, surprising behaviour is again observed as the corresponding solution converges to a repelling periodic orbit defining the basin boundary of the final base state; see the blue trajectory.

185 ## 5   Rate-induced tipping in power grid networks

R-tipping instabilities are not confined to natural systems, but can occur in any system, including human systems. One example is the energy sector and power grid networks (Suchithra et al., 2020). Crucially, electricity needs to be used as soon as it is produced since it cannot be stored easily (Mokrian et al., 2006). Therefore, providing a near constant voltage of electricity to millions of homes, while power demand varies seasonally, daily, and may spike during major events, is a technological

190 challenge (Mahmud and Zahedi, 2016). Some noticeable examples of power blackouts or near misses are: the Northeast USA blackout in 2003 caused by a series of faults in local control systems (Hu et al., 2016); and the near miss blackout in England following the conclusion of the Euro 1990 semi-final (Swarup, 2007).

Here, we use a conceptual model of a power grid network (Dobson et al., 1988; Dobson and Chiang, 1989; Budd and Wilson, 2002), where changing power demand plays the role of external forcing. The situation with stable states in this model is more

195 complicated than in the previous examples. The power demand changes within a range where there are infinitely many stable equilibria with the same fixed voltage magnitude and a 2π difference in the phase angle; see Methods for details. These stable equilibria are the base states of the system. Furthermore, there are two alternative states. An *alternative transient state* is a temporary drop in the voltage magnitude accompanied by a 2π shift in the phase angle. This state corresponds to a transition between two neighbouring base states. An *alternative stable state* is at zero voltage magnitude, and corresponds to electrical

200 blackout.[2]

We now demonstrate that a rapid increase in power demand can lead to R-tipping in the form of different disruptions in power supply. First, we note that for slow enough increases in power demand, the power grid network always tracks the moving base state (not shown here). Then, in Figure 5, we show the response of the power grid network to different forms of increase in power demand with higher rates of change. We start with three ramp shifts that vary between the same levels of power demand,

205 without crossing any critical levels, but at different rates. These are given by a concatenation of the left half of a colour curve and the black dashed curve in Figure 5(a). Owing to the higher rates of change, all three ramp shifts cause R-tipping to the alternative stable state, resulting in blackout; see the dashed curves in Figure 5(b). However, reversing the power demand (see solid colour pulses in Figure 5(a)) can avoid blackout and restore the power grid network to one of its base states if the reversal is fast enough (see the corresponding solid colour responses in Figure 5(b)). The slowest (blue) reversal is too slow to avoid

---

[2]In the model, the voltage drops to negative infinity, but we restrict to physically relevant non-negative voltage magnitudes.
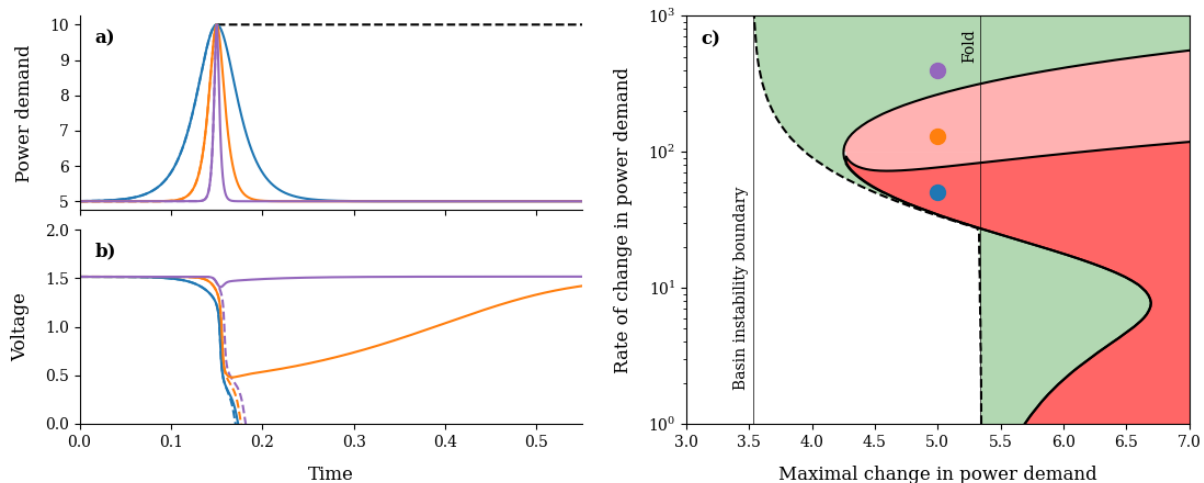
Figure 5. Tipping for ramp and return profiles in the power grid model. Time series of power demand (a) and voltage (b) for ramp (dashed) and return (solid) power demand profiles. Power demand profiles vary between the same minimum and maximum levels but at different rates: slow (blue), medium (orange) and fast (purple). (c) Tipping diagram of ramp and return profiles. Critical boundaries separate regions of tracking from tipping (blackout) for both, the ramp profile (black dashed curve) and for return profile (black solid curve). For return profiles reversible tipping is also possible through a phase slip. White region: tracking for ramp and return profiles; green region: tipping to blackout for ramp profiles, tracking for return profiles; red regions: tipping to blackout for ramp profiles, tipping to phase slips (light red region) and tipping to blackouts (dark red region) for return profiles.

210 *irreversible R-tipping* to blackout. The medium-rate (orange) reversal avoids blackout, but involves *reversible R-tipping* to the alternative transient state - a temporary voltage drop followed by a long recovery towards a base state. The fastest (purple) reversal avoids both types of R-tipping and does not cause any noticeable disruptions to power supply.

The tipping diagram for ramp and return forcing profiles in Figure 5(c) has, in addition to multiple critical rates already observed in the previous examples, an important new feature. Owing to multiple base states, there are two different red regions

215 corresponding to two different types of R-tipping for return forcing profile: irreversible R-tipping to blackout (dark red region) where the voltage collapses permanently, and reversible R-tipping to the neighbouring base state (light red region) involving a temporary voltage drop and a 2π phase slip. The three scenarios illustrated in Figure 5(a) and (b) correspond to the three coloured dots in the tipping diagram in Figure 5(c). Note that all three dots are located past the basin instability boundary and below the critical level of power demand (indicated by the black vertical Fold line), meaning that these transitions are purely

220 rate-induced.

6 Conclusions

We have shown that many natural and human systems can experience rate-induced tipping (R-tipping). Such instabilities usually occur for sufficiently fast increases in external forcing, and despite never crossing any critical levels of external forcing.

In other words, systems are able to continually adapt to a moving base state and therefore avoid tipping when external forcing
225   increases slow enough, but fail to adapt to or track a moving base state when external forcing increases faster than some
critical rate. Reversing the external forcing can prevent a system from suffering R-tipping but the rates required for this add
an additional layer of complexity in the presence of bifurcation-induced tipping (B-tipping). Previously, it has been shown that
safe overshoots of critical levels for bifurcation-induced tipping require fast rates of change (Ritchie et al., 2021). However,
faster rates of change make a system more susceptible to R-tipping. To make the concept of R-tipping accessible to a wide
230   scientific audience, we:

- Give an easily verifiable criterion of threshold instability, and basin instability, for R-tipping to occur.

- Demonstrate basin instability and ensuing R-tipping in conceptual models of natural and human systems, including
  irreversible and reversible R-tipping.

- Highlight interesting phenomena, such as multiple critical rates and return tipping, that can arise from an interplay
235   between R-tipping and B-tipping for non-monotone forcing.

The models used in this study, for representing a predator-prey ecosystem, the Atlantic overturning circulation and an
electrical power grid network, are relatively simple. Since our forcing profiles are very idealised by design, we focus on
the qualitative behaviour that can arise for different rates of forcing rather than on quantitative predictions. For this, further
research on R-tipping is required in more-realistic higher-complexity models, such as state-of-the-art global circulation models.
240   The base state in such models may not necessarily be a steady state (an equilibrium), but for example could take the form of
a periodic orbit or even a chaotic state. This could lead to more complex tipping behaviour, such as phase tipping (Alkhayuon
and Ashwin, 2018; Kaszás et al., 2019; Alkhayuon et al., 2021; Ashwin and Newman, 2021; Alkhayuon et al., 2022).

R-tipping is likely to be prevalent in many systems given contemporary rates of change such as unprecedented anthropogenic
climate change. This review highlights the importance of considering how fast external forcing is changing as opposed to
245   solely focusing on magnitudes of change. Consequently, the actions taken to control the rate of change in forcing are equally
as important as the actions taken to control the level at which forcing is halted.

Methods

Forcing profiles

In our analysis we consider two types of nonlinear external forcing, $\lambda(t)$. The first is a *monotonic ramp*, where the forcing
250   starts close to the minimum level λ_-, and subsequently increases continuously until reaching a maximal level, $\lambda_- + \Delta_\lambda$, at
time T. The forcing subsequently remains at this maximal level and therefore Δ_λ defines the maximal change in the forcing:

$$\lambda(t) = \begin{cases} \lambda_- + \Delta_\lambda \operatorname{sech}\big(r(t-T)\big), & t \leq T, \\ \lambda_- + \Delta_\lambda, & t > T. \end{cases} \tag{1}$$

For R-tipping scenarios with a fixed maximal change, Δ_λ, how fast the forcing changes, governed by r, determines if tipping occurs.

255   Additionally, we consider the possibility of avoiding tipping by reversing the forcing, with a *non-monotonic return* trajectory. Equation (1) is modified by removing the piecewise element of the forcing for $t > T$, such that the forcing returns back to its initial level (at a mirrored rate of the approach) after reaching the maximal level, $\lambda_- + \Delta_\lambda$, at time T:

$$\lambda(t) = \lambda_- + \Delta_\lambda \operatorname{sech}(r(t-T)). \tag{2}$$

Trajectories of the form of equation (2) provide idealised scenarios such as the future development of technologies to remove
260   CO_2 from the atmosphere and reverse the impact of anthropogenic climate change back to initial levels (Huntingford et al., 2017).

Plant-herbivore model

The time evolution of plant, P, and herbivore, H, biomass densities [g/m^2] can be modelled as two coupled ordinary differential equations (Scheffer et al., 2008; O'Keeffe and Wieczorek, 2020).

265    $$\frac{dP}{dt} = \rho(t)P - CP^2 - H\,g(P), \tag{3}$$

$$\frac{dH}{dt} = H\big(Ee^{-bP}\,g(P) - m(t)\big), \tag{4}$$

with a functional response

$$g(P) = c_{\max}\frac{P^2}{P^2 + a^2}e^{-b_c P}. \tag{5}$$

Following the approach of (O'Keeffe and Wieczorek, 2020), we fix six of the eight parameters (see Table 2.1 Ref. (O'Keeffe
270   and Wieczorek, 2020)) and allow the plant growth rate $\rho(t)$ [1/day] and herbivore mortality rate $m(t)$ [1/day] to vary over time subject to environmental conditions. We assume that environmental conditions, $\nu(t)$, is a dimensionless time variable that takes the form of the monotonic ramp, Eq. (1). Furthermore, we assume that plant growth rate, $\rho(t)$, and herbivore mortality rate, $m(t)$, increase linearly in response to increasing environmental conditions as described by the following:

$$\rho(t) = \rho_- + \Delta_\rho\nu(t), \tag{6}$$

275    $$m(t) = m_- + \Delta_m\nu(t), \tag{7}$$

where ρ_- and m_- are the initial values, Δ_ρ and Δ_m are the maximum changes in plant growth rate and herbivore mortality rate respectively.

AMOC model

Wood et al. (2019) proposed a five-box model to model the global oceanic current. The model is driven by salinity fluxes [psu], S_i, in the main ocean waters: the North Atlantic (N), Tropical Atlantic (T), Indo-Pacific (IP), Southern Ocean (S) and Bottom waters (B). The flow strength, q [Sv], of the Atlantic Meridional Overturning Circulation (AMOC) is subsequently determined by a (fixed) temperature gradient, ΔT, and variable salinity gradient, $\Delta S = S_N - S_S$, between the North Atlantic and Southern Ocean boxes:

$$q = \frac{\lambda(\alpha\Delta T + \beta\Delta S)}{1 + \lambda\alpha\mu}. \tag{8}$$

Alkhayuon et al. (2019) empirically highlighted that the salinity of the Southern Ocean and Bottom waters, vary much slower than the other boxes. Therefore, assuming these salinities are fixed and the salinity in the Indo-Pacific, S_{IP}, can be determined from a conservation of salinity, the model reduces to the following two dimensional model:

$$V_N \frac{dS_N}{dt} = q(S_T - S_N) + K_N(S_T - S_N) - F_N(t)S_0, \tag{9}$$

$$V_T \frac{dS_T}{dt} = q[\gamma S_S + (1-\gamma)S_{IP} - S_T] + K_S(S_S - S_T) + K_N(S_N - S_T) - F_T(t)S_0, \tag{10}$$

for $q \geq 0$ and

$$V_N \frac{dS_N}{dt} = |q|(S_B - S_N) + K_N(S_T - S_N) - F_N(t)S_0, \tag{11}$$

$$V_T \frac{dS_T}{dt} = |q|(S_N - S_T) + K_S(S_S - S_T) + K_N(S_N - S_T) - F_T(t)S_0, \tag{12}$$

for $q < 0$. For more details about the parameters and their values we refer the reader to Tables 3 and 4 in Ref. (Alkhayuon et al., 2019).

In this study we are interested in the surface freshwater fluxes F_i [Sv], i in $\{N, T, IP, S\}$ as input parameters for the system. Following the approach of (Alkhayuon et al., 2019; Wood et al., 2019) these fluxes are defined as linear functions of a hosing parameter H [Sv] such that: the total flux is 0 for all H, and $H = 0$ corresponds to the baseline values of F_i (Table 3 Ref.(Alkhayuon et al., 2019)).

$$F_N(t) = 0.486 + 0.1311\,H(t), \tag{13}$$

$$F_T(t) = -0.997 + 0.6961\,H(t), \tag{14}$$

$$F_{IP}(t) = -0.754 - 0.5646\,H(t), \tag{15}$$

$$F_S(t) = 1.265 - 0.2626\,H(t). \tag{16}$$

The hosing parameter $H(t)$ is assumed to be increasing monotonically from 0 to $\Delta_H > 0$ according to Eq. (1).

The power grid model

305 We use a 3-bus power system model from (Dobson et al., 1988; Dobson and Chiang, 1989) to represent the dynamics that can
be observed on a power gird. Two generators supply power to a P-Q load in parallel with a capacitor and induction motor (Revel
et al., 2006). The model consists of four differential equations for the generator phase angle, δ_m, and angular velocity, ω_m, and
the phase angle, δ and magnitude, V, of the load voltage (Ajjarapu and Lee, 1992):

$$
\begin{aligned}
\dot{\delta}_m &= \omega_m, \\
\dot{\omega}_m &= \frac{1}{M}\big(-d_m\omega_m + P_m - P_e\big), \\
\dot{\delta} &= \frac{1}{K_{q\omega}}\big(-K_{qv}V - K_{qv^2}V^2 + Q_l - Q_0 - Q_1\big), \\
\dot{V} &= \frac{1}{TK_{q\omega}K_{pv}}\big(K_{p\omega}K_{qv^2}V^2 + (K_{p\omega}K_{qv} - K_{q\omega}K_{pv})V \\
&\quad + K_{p\omega}(Q_0 + Q_1 - Q_l) - K_{q\omega}(P_0 + P_1 - P_l)\big).
\end{aligned}
\tag{17}
$$

310 where P_e, P_l and Q_l are given by

$$
\begin{aligned}
P_l &= -V_0 V T_0 \sin(\delta + \theta_0) - V_m V Y_m \sin(\delta - \delta_m + \theta_m) + (Y_0 \sin(\theta_0) + Y_m sin(\theta_m))V^2, \\
Q_l &= V_0 V Y_0 cos(\delta + \theta_0) + V_m V Y_m \cos(\delta - \delta_m + \theta_m) - (Y_0 \cos(\theta_0) + Y_m \cos(\theta_m))V^2) \\
P_e &= -V_m V Y_m \sin(\delta - \delta_m \theta_m) - V_m^2 Y_m \sin(\theta_m).
\end{aligned}
\tag{18}
$$

For a full description of parameters and the values used in this study, we refer the reader to (Budd and Wilson, 2002). However,
we choose to set $P_1 = 5$, the real power demand of the load, such that when Q_1, the reactive power demand (referred to power
demand in the main text) of the load, is varied, according to either Eq. (1) or Eq (2), the system can only cross a fold bifurcation
315 and does not encounter a Hopf bifurcation as observed for $P_1 = 0$ (Wang et al., 1994).

Code availability. The codes used to conduct simulations and generate figures are available via the GitHub repository (Ritchie et al., 2022).

Video supplement. supplementary videos are available via the GitHub repository (Ritchie et al., 2022).

Competing interests. There are no competing interests

Acknowledgements. P.R. and P.C. research was funded by the European Research Council 'Emergent Constraints on Climate-Land feedbacks
320   in the Earth System (ECCLES)' project, grant agreement number 742472. H.A. and S.W. research was funded by Enterprise Ireland grant
no. 20190771.

References

V. Ajjarapu and B. Lee. Bifurcation theory and its application to nonlinear dynamical phenomena in an electrical power system. *IEEE Transactions on Power Systems*, 7(1):424–431, 1992.

325 H. Alkhayuon, P. Ashwin, L. C. Jackson, C. Quinn, and R. A. Wood. Basin bifurcations, oscillatory instability and rate-induced thresholds for atlantic meridional overturning circulation in a global oceanic box model. *Proceedings of the Royal Society A*, 475(2225):20190051, 2019.

H. Alkhayuon, R. C. Tyson, and S. Wieczorek. Phase tipping: how cyclic ecosystems respond to contemporary climate. *Proceedings of the Royal Society A*, 477(2254):20210059, 2021.

330 H. Alkhayuon, J. Marley, S. Wieczorek, and R. C. Tyson. Stochastic resonance in climate reddening increases the risk of cyclic ecosystem extinction via phase-tipping. *arXiv preprint arXiv:2210.02797*, 2022.

H. M. Alkhayuon and P. Ashwin. Rate-induced tipping from periodic attractors: Partial tipping and connecting orbits. *Chaos: An Interdisciplinary Journal of Nonlinear Science*, 28(3):033608, 2018.

P. Arias, N. Bellouin, E. Coppola, R. Jones, G. Krinner, J. Marotzke, V. Naik, M. Palmer, G.-K. Plattner, J. Rogelj, et al. Climate change

335 2021: The physical science basis. contribution of working group i to the sixth assessment report of the intergovernmental panel on climate change; technical summary. 2021.

P. Ashwin and J. Newman. Physical invariant measures and tipping probabilities for chaotic attractors of asymptotically autonomous systems. *The European Physical Journal Special Topics*, 230(16):3235–3248, 2021.

P. Ashwin and A. S. von der Heydt. Extreme sensitivity and climate tipping points. *Journal of Statistical Physics*, 179(5):1531–1552, 2020.

340 P. Ashwin, S. Wieczorek, R. Vitolo, and P. Cox. Tipping points in open systems: bifurcation, noise-induced and rate-dependent examples in the climate system. *Philosophical Transactions of the Royal Society A: Mathematical, Physical and Engineering Sciences*, 370(1962): 1166–1184, 2012.

C. Budd and J. Wilson. Bogdanov-takens bifurcation points and sil'nikov homoclinicity in a simple power-system model of voltage collapse. *IEEE Transactions on Circuits and Systems I: Fundamental Theory and Applications*, 49(5):575–590, 2002.

345 J. Clarke, C. Huntingford, P. Ritchie, and P. Cox. The compost bomb instability in the continuum limit. *The European Physical Journal Special Topics*, 230(16):3335–3341, 2021.

V. Dakos, B. Matthews, A. P. Hendry, J. Levine, N. Loeuille, J. Norberg, P. Nosil, M. Scheffer, and L. De Meester. Ecosystem tipping points in an evolving world. *Nature ecology & evolution*, 3(3):355–362, 2019.

I. Dobson and H.-D. Chiang. Towards a theory of voltage collapse in electric power systems. *Systems & Control Letters*, 13(3):253–262,

350 1989.

I. Dobson, H.-D. Chiang, J. S. Thorp, and L. Fekih-Ahmed. A model of voltage collapse in electric power systems. In *Proceedings of the 27th IEEE Conference on Decision and Control*, pages 2104–2109. IEEE, 1988.

L. Halekotte and U. Feudel. Minimal fatal shocks in multistable complex networks. *Scientific reports*, 10(1):1–13, 2020.

K. Hill, J. Zanetell, and J. A. Gemmer. Most probable transition paths in piecewise-smooth stochastic differential equations. *Physica D:*

355 *Nonlinear Phenomena*, 439:133424, 2022.

X.-B. Hu, A. V. Gheorghe, M. S. Leeson, S. Leng, J. Bourgeois, and X. Qu. Risk and safety of complex network systems, 2016.

C. Huntingford, H. Yang, A. Harper, P. M. Cox, N. Gedney, E. J. Burke, J. A. Lowe, G. Hayman, W. J. Collins, S. M. Smith, et al. Flexible parameter-sparse global temperature time profiles that stabilise at 1.5 and 2.0° c. *Earth System Dynamics*, 8(3):617–626, 2017.

B. Kaszás, U. Feudel, and T. Tél. Tipping phenomena in typical dynamical systems subjected to parameter drift. *Scientific reports*, 9(1): 1–12, 2019.

T. Kaur and P. Sharathi Dutta. Critical rates of climate warming and abrupt collapse of ecosystems. *Proceedings of the Royal Society A*, 478 (2264):20220086, 2022.

C. Kiers and C. K. Jones. On conditions for rate-induced tipping in multi-dimensional dynamical systems. *Journal of Dynamics and Differential Equations*, 32(1):483–503, 2020.

C. Kuehn. A mathematical framework for critical transitions: Bifurcations, fast–slow systems and stochastic dynamics. *Physica D: Nonlinear Phenomena*, 240(12):1020–1035, 2011.

C. Kuehn and I. P. Longo. Estimating rate-induced tipping via asymptotic series and a melnikov-like method. *Nonlinearity*, 35(5):2559, 2022.

N. Lacetera. Impact of climate change on animal health and welfare. *Animal Frontiers*, 9(1):26–31, 2019.

T. M. Lenton. Early warning of climate tipping points. *Nature climate change*, 1(4):201–209, 2011.

T. M. Lenton, H. Held, E. Kriegler, J. W. Hall, W. Lucht, S. Rahmstorf, and H. J. Schellnhuber. Tipping elements in the earth's climate system. *Proceedings of the national Academy of Sciences*, 105(6):1786–1793, 2008.

J. Lohmann and P. D. Ditlevsen. Risk of tipping the overturning circulation due to increasing rates of ice melt. *Proceedings of the National Academy of Sciences*, 118(9), 2021.

J. Lohmann, D. Castellana, P. D. Ditlevsen, and H. A. Dijkstra. Abrupt climate change as a rate-dependent cascading tipping point. *Earth System Dynamics*, 12(3):819–835, 2021.

I. P. Longo, C. Núñez, R. Obaya, and M. Rasmussen. Rate-induced tipping and saddle-node bifurcation for quadratic differential equations with nonautonomous asymptotic dynamics. *SIAM Journal on Applied Dynamical Systems*, 20(1):500–540, 2021.

C. Luke and P. Cox. Soil carbon and climate change: from the jenkinson effect to the compost-bomb instability. *European Journal of Soil Science*, 62(1):5–12, 2011.

N. Mahmud and A. Zahedi. Review of control strategies for voltage regulation of the smart distribution network with high penetration of renewable distributed generation. *Renewable and Sustainable Energy Reviews*, 64:582–595, 2016.

M. I. Maturana, C. Meisel, K. Dell, P. J. Karoly, W. D'Souza, D. B. Grayden, A. N. Burkitt, P. Jiruska, J. Kudlacek, J. Hlinka, et al. Critical slowing down as a biomarker for seizure susceptibility. *Nature communications*, 11(1):1–12, 2020.

M. U. Mirza, A. Richter, E. H. van Nes, and M. Scheffer. Technology driven inequality leads to poverty and resource depletion. *Ecological Economics*, 160:215–226, 2019.

P. Mokrian, M. Stephen, et al. A stochastic programming framework for the valuation of electricity storage. In *26th USAEE/IAEE North American Conference*, pages 24–27. Citeseer, 2006.

F. K. Neijnens, K. Siteur, J. van de Koppel, and M. Rietkerk. Early warning signals for rate-induced critical transitions in salt marsh ecosystems. *Ecosystems*, 24(8):1825–1836, 2021.

P. E. O'Keeffe and S. Wieczorek. Tipping phenomena and points of no return in ecosystems: beyond classical bifurcations. *SIAM Journal on Applied Dynamical Systems*, 19(4):2371–2402, 2020.

E. O'Sullivan, S. Wieczorek, and K. Mulchrone. Rate-induced tipping to metastable zombie fires. *Unpublished preprint*, 2022.

P. B. Reich, S. E. Hobbie, and T. D. Lee. Plant growth enhancement by elevated co2 eliminated by joint water and nitrogen limitation. *Nature Geoscience*, 7(12):920–924, 2014.

G. Revel, D. M. Alonso, and J. L. Moiola. Bifurcation analysis in a power system model. *IFAC Proceedings Volumes*, 39(8):303–308, 2006.

P. Ritchie and J. Sieber. Early-warning indicators for rate-induced tipping. *Chaos: An Interdisciplinary Journal of Nonlinear Science*, 26(9): 093116, 2016.

P. Ritchie, Ö. Karabacak, and J. Sieber. Inverse-square law between time and amplitude for crossing tipping thresholds. *Proceedings of the Royal Society A*, 475(2222):20180504, 2019.

P. Ritchie, H. Alkhayuon, P. Cox, and S. Wieczorek. Rate-induced tipping in natural and human systems. *GitHub Repository*, github.com/hassanalkhayuon/rtippingreview, 2022.

P. D. Ritchie, J. J. Clarke, P. M. Cox, and C. Huntingford. Overshooting tipping point thresholds in a changing climate. *Nature*, 592(7855): 517–523, 2021.

M. Scheffer. Foreseeing tipping points. *Nature*, 467(7314):411–412, 2010.

M. Scheffer, E. H. Van Nes, M. Holmgren, and T. Hughes. Pulse-driven loss of top-down control: the critical-rate hypothesis. *Ecosystems*, 11(2):226–237, 2008.

M. Scheffer, J. Bascompte, W. A. Brock, V. Brovkin, S. R. Carpenter, V. Dakos, H. Held, E. H. Van Nes, M. Rietkerk, and G. Sugihara. Early-warning signals for critical transitions. *Nature*, 461(7260):53–59, 2009.

K. Siteur, M. B. Eppinga, A. Doelman, E. Siero, and M. Rietkerk. Ecosystems off track: rate-induced critical transitions in ecological models. *Oikos*, 125(12):1689–1699, 2016.

K. Slyman and C. K. Jones. Rate and noise-induced tipping working in concert. *arXiv preprint arXiv:2210.00873*, 2022.

K. Suchithra, E. Gopalakrishnan, E. Surovyatkina, and J. Kurths. Rate-induced transitions and advanced takeoff in power systems. *Chaos: An Interdisciplinary Journal of Nonlinear Science*, 30(6):061103, 2020.

B. Swarup. Energy storage takes off. *Physics world*, 20(7):42, 2007.

J. M. T. Thompson and J. Sieber. Climate tipping as a noisy bifurcation: a predictive technique. *IMA Journal of Applied Mathematics*, 76 (1):27–46, 2011.

J. M. T. Thompson, H. Stewart, and Y. Ueda. Safe, explosive, and dangerous bifurcations in dissipative dynamical systems. *Physical Review E*, 49(2):1019, 1994.

B. van der Bolt and E. H. van Nes. Understanding the critical rate of environmental change for ecosystems, cyanobacteria as an example. *PloS one*, 16(6):e0253003, 2021.

B. van der Bolt, E. H. van Nes, S. Bathiany, M. E. Vollebregt, and M. Scheffer. Climate reddening increases the chance of critical transitions. *Nature Climate Change*, 8(6):478–484, 2018.

A. Vanselow, S. Wieczorek, and U. Feudel. When very slow is too fast-collapse of a predator-prey system. *Journal of theoretical biology*, 479:64–72, 2019.

A. Vanselow, L. Halekotte, and U. Feudel. Evolutionary rescue can prevent rate-induced tipping. *Theoretical Ecology*, 15(1):29–50, 2022.

H. O. Wang, E. H. Abed, and A. M. Hamdan. Bifurcations, chaos, and crises in voltage collapse of a model power system. *IEEE Transactions on Circuits and Systems I: Fundamental Theory and Applications*, 41(4):294–302, 1994.

S. Wieczorek, P. Ashwin, C. M. Luke, and P. M. Cox. Excitability in ramped systems: the compost-bomb instability. *Proceedings of the Royal Society A: Mathematical, Physical and Engineering Sciences*, 467(2129):1243–1269, 2011.

S. Wieczorek, C. Xie, and P. Ashwin. Rate-induced tipping: Thresholds, edge states and connecting orbits. *arXiv preprint arXiv:2111.15497*, 2021.

D. Witthaut, F. Hellmann, J. Kurths, S. Kettemann, H. Meyer-Ortmanns, and M. Timme. Collective nonlinear dynamics and self-organization in decentralized power grids. *Reviews of Modern Physics*, 2021.

435   R. A. Wood, J. M. Rodríguez, R. S. Smith, L. C. Jackson, and E. Hawkins. Observable, low-order dynamical controls on thresholds of the
      atlantic meridional overturning circulation. *Climate Dynamics*, 53(11):6815–6834, 2019.